

# Magnetic moments of octet baryons in hot and dense nuclear matter

Harpreet Singh<sup>1)</sup> Arvind Kumar<sup>2)</sup> Harleen Dahiya<sup>3)</sup>

Department of Physics, Dr. B R Ambedkar National Institute of Technology Jalandhar, Jalandhar – 144011, Punjab, India

**Abstract:** We have calculated the in-medium magnetic moments of octet baryons in the presence of hot and dense symmetric nuclear matter. Effective magnetic moments of baryons have been derived from medium modified quark masses within the chiral  $SU(3)$  quark mean field model. Further, for better insight into the medium modification of baryonic magnetic moments, we have considered the explicit contributions from the valence quarks, sea quarks and the sea orbital angular momentum of sea quarks. These effects have been successful in giving the description of baryonic magnetic moments in vacuum. The magnetic moments of baryons are found to vary significantly as a function of density of nuclear medium.

**Keywords:** nuclear matter, magnetic moments, heavy ion collisions

**PACS:** 14.40.Lb, 14.40.Nd **DOI:** 10.1088/1674-1137/41/9/094104

## 1 Introduction

The study of in-medium properties of octet and decuplet baryons is of great importance in the present era. Heavy-ion collision experiments at various experimental facilities such as the LHC at CERN [1], FSI at EMC [2], CBM at FAIR [3], etc., are focused on the study of matter in free space as well as in the presence of a medium. A major goal of modern hadron accelerator facilities is to investigate the structure of hadrons by scattering experiments at large momentum transfer, typically  $1 \text{ GeV}/c^2$  and beyond, so as to map out various internal charge distributions underlying quark and gluon degrees of freedom. The main objectives of the heavy-ion collision facilities are to study the properties of hadrons in hadronic matter, chiral symmetry restoration at high temperature and density of medium, and the de-confinement phase from hadrons to quark-gluon plasma (QGP), and to determine the equation of state for hadronic matter at high density [4–6]. The experiments at various facilities, besides the data, also require theoretical insight into the hadronic properties, such as magnetic moment, charge radii, and electromagnetic form factors.

The magnetic moment of the particle plays an important role in the study of structure of matter at the sub-nuclear level, as it largely depends upon its structure and structure parameters. Theoretically, the magnetic moments of octet as well as decuplet baryons have been ex-

tensively studied in free space [7–13]. Constituent quark model studies proposed that the baryonic magnetic moments can be calculated by summing the magnetic moments of constituent quarks [14, 15]. However, the values so obtained differ from those obtained experimentally.

The magnetic moments of the octet baryons have been calculated from the structure parameters of baryons, such as electromagnetic form factors [16]. They are derived from the magnetic form factor  $G_m(Q^2)$  at  $Q^2=0$  (where  $Q^2$  is the squared four-momentum of the baryon) [17]. They have also been extrapolated from the study of charge radii [19] and medium-modified masses of the baryons [20]. Covariant baryon chiral perturbation theory [21, 22] has been extensively used to study octet baryon magnetic moments using the idea of  $SU(3)$  symmetry breaking. It has been shown that in the low energy regime the chiral expansion of octet baryon magnetic moments is possible if one considers the correction terms, such as loop corrections and decuplet degrees of freedom, to be small [23–29]. However, in order to gain a deeper insight into the underlying quark dynamics, it is useful to consider the individual quark contribution to baryonic magnetic moments. The MIT bag model provided a useful way to calculate baryonic magnetic moments considering the constituent quarks to be non-interacting [16]. Later, weak coupling between the constituent quarks was proposed to include the interactions of quarks in the baryons [18]. The observed ratio of con-

Received 24 April 2017

1) E-mail: harpreetmscdav@gmail.com

2) E-mail: iitd.arvind@gmail.com, kumara@nitj.ac.in

3) E-mail: dahiyah@nitj.ac.in



Content from this work may be used under the terms of the Creative Commons Attribution 3.0 licence. Any further distribution of this work must maintain attribution to the author(s) and the title of the work, journal citation and DOI. Article funded by SCOAP<sup>3</sup> and published under licence by Chinese Physical Society and the Institute of High Energy Physics of the Chinese Academy of Sciences and the Institute of Modern Physics of the Chinese Academy of Sciences and IOP Publishing Ltd

tributions from  $u$ -quarks to contributions from  $d$ -quarks in the calculation of the total magnetic moment of the nucleon by this approach can only be justified by considering dynamical quark masses [17]. Thus, one has to consider constituent quark masses in place of current quark masses to study baryonic magnetic moments including quark dynamics. This is strong evidence of the presence of relativistic and gluon effects which are not accounted for in conventional quark models.

Besides the free space calculations of baryonic structural properties (such as magnetic moments), the medium modification of these properties has always been an interesting aspect of QCD studies. A deep inelastic muon-nucleus scattering experiment at EMC has indicated that nucleon properties in the nuclear medium can be different from their vacuum values [30]. Similarly, the magnetic moment of the proton in  $^{12}\text{C}$  seemed to be enhanced by about 25% in nuclear medium as compared to its value in free space [31].

Theoretical models for nuclear matter, such as the Walecka model [32], sigma model [33], non-linear sigma model [34], Zimanyi and Moszkowski model [35], cloudy bag model [36], Nambu-Jona-Lasinio (NJL) model [37], etc., have successfully explained several properties of nuclear matter [38, 39]. The key to success of models like the NJL model in explaining low energy baryonic dynamics is the assumption of hadrons having chiral quarks and interaction between the constituent quarks [40]. For better understanding of baryon properties in quark degrees of freedom, chiral quark models such as the quark meson coupling (QMC) model were developed along similar lines as the NJL model and cloudy bag model [41]. Medium modification of magnetic moments of octet baryons has been calculated using the QMC model [48]. The QMC model has been used at finite temperature and baryonic density, and medium modification of magnetic moments of baryons has been derived through medium modification of the bag radius. The results are quite close to the experimental data for the vacuum values.

In the present work we have used the chiral  $SU(3)$  quark mean field model to calculate the in-medium magnetic moments of the baryon octet at finite temperature and density of the medium through the medium modification of baryon masses. The relation of baryon magnetic moments and corresponding effective quark masses has been derived in the analysis of hyperon static properties [49]. We will follow similar relations to obtain medium-modified values of magnetic moments of baryons. The chiral  $SU(3)$  quark mean field model (CQMF) [34, 41, 52, 53] has been extended from the quark mean field model [42], which is based on the QMC model approach. In this model, the mean field approximation is used, which uses classical expectation values

in place of quantum field operators [43]. The quarks are assumed to be constituent quarks, which are confined in the baryons by a confining potential. Finite nuclei properties have been studied in this model and reasonably good results have been obtained [41]. Within the CQMF model, the in-medium masses of quarks and hence baryons are calculated through the medium modification of scalar iso-scalar fields  $\sigma$  and  $\zeta$  and the scalar dilaton field  $\chi$  [34, 41, 52, 53].

Beside the interaction of scalar meson fields, some entities with the characteristics of Goldstone bosons (GB) play a major role in the interaction of quarks and their magnetic moments [44]. If we assume Goldstone bosons in the interior of hadrons, we will have different propagation properties of the states [14]. Spin-dependent features of the hadronic spectrum can be successfully explained by considering internal GB exchange between the quarks. Further, the significant spin-orbit coupling contribution can also be accounted for by this approach. Beside this, the violation of the Gottfried sum rule leads to isospin-asymmetric sea quarks in baryons, and sea quark contributions should also be considered in the magnetic moments of baryons [10, 45–47]. In this work we have considered GB exchange in the interior of baryons, and have also considered the contribution from sea quarks. These two effects can further modify the effective magnetic moments.

The outline of the paper is as follows. In Section 2.1 we will apply the CQMF model to find the effective quark masses at finite temperature and density of nuclear medium, and hence, calculate effective baryon octet masses. We will discuss the effect of valence quarks, sea quarks and orbital angular momentum of sea quarks on the magnetic moments of baryons in Section 2.2. Section 3 is devoted to numerical calculations and results. Section 4 gives a summary of the present work.

## 2 Model

### 2.1 Chiral $SU(3)$ quark mean field model for quark masses

To study the structure of hadrons in the chiral limit and explore it in quark degrees of freedom, the quarks are divided into two types, left-handed ' $q_L$ ' and right-handed ' $q_R$ '. Under  $SU(3)_L \times SU(3)_R$  transformation, the corresponding transformations for the left- and right-handed quarks are

$$q_L \rightarrow q'_L = L q_L, \quad q_R \rightarrow q'_R = R q_R, \quad (1)$$

where ' $L$ ' and ' $R$ ' are global  $SU(3)_L \times SU(3)_R$  transformations given as

$$L(\alpha_L) = \exp \left[ i \sum_{a=0}^8 \alpha_L^a \lambda_{La} \right], \quad R(\alpha_R) = \exp \left[ i \sum_{b=0}^8 \alpha_R^b \lambda_{Rb} \right], \quad (2)$$

$\alpha_L$  and  $\alpha_R$  represent space-time independent parameters with indices ( $a=0,\dots,8$ ) and ( $b=0,\dots,8$ ).  $\lambda_L$  and  $\lambda_R$  are Gell-Mann matrices written as

$$\lambda_L = \lambda \frac{(1-\gamma_5)}{2}, \quad \lambda_R = \lambda \frac{(1+\gamma_5)}{2}. \quad (3)$$

The nonets of spin-0 scalar ( $\Sigma$ ) and pseudoscalar ( $\Pi$ ) mesons can be written in compact form using Gell-Mann matrices as

$$M(M^\dagger) = \Sigma \pm i\Pi = \frac{1}{\sqrt{2}} \sum_{a=0}^8 (s_a \pm i p_a) \lambda_a, \quad (4)$$

where  $\lambda_a$  are Gell-Mann matrices with  $\lambda_0 = \sqrt{\frac{2}{3}}I$ , and  $s_a$  and  $p_a$  are the nonets of scalar and pseudoscalar mesons, respectively. The plus and minus signs are for  $M$  and  $M^\dagger$ , respectively, which transform under chiral  $SU(3)$  transformation as

$$M \rightarrow M' = LMR^\dagger, \quad (5)$$

$$M^\dagger \rightarrow M'^\dagger = RM^\dagger L^\dagger. \quad (6)$$

In a similar way, spin-1 mesons are defined by

$$l_\mu(r_\mu) = \frac{1}{2} (V_\mu \pm A_\mu) = \frac{1}{2\sqrt{2}} \sum_{a=0}^8 (v_\mu^a \pm a_\mu^a) \lambda_a, \quad (7)$$

where  $v_\mu^a$  and  $a_\mu^a$  are nonets of vector and pseudovector mesons respectively. The alternative plus and minus signs are for  $l_\mu$  and  $r_\mu$  respectively, and will transform under chiral  $SU(3)$  transformation as

$$l_\mu \rightarrow l'_\mu = L l_\mu L^\dagger, \quad (8)$$

$$r_\mu \rightarrow r'_\mu = R r_\mu R^\dagger. \quad (9)$$

The physical states for scalar and vector mesons are explicitly represented as

$$\Sigma = \frac{1}{\sqrt{2}} \sum_{a=0}^8 s_a \lambda_a = \begin{pmatrix} \frac{1}{\sqrt{2}}(\sigma + a_0^0) & a_0^+ & \kappa^{*+} \\ a_0^- & \frac{1}{\sqrt{2}}(\sigma - a_0^0) & \kappa^{*0} \\ \kappa^{*-} & \bar{\kappa}^{*0} & \zeta \end{pmatrix}, \quad (10)$$

and

$$V_\mu = \frac{1}{\sqrt{2}} \sum_{a=0}^8 v_\mu^a \lambda_a = \begin{pmatrix} \frac{1}{\sqrt{2}}(\omega_\mu + \rho_\mu^0) & \rho_\mu^+ & K_\mu^{*+} \\ \rho_\mu^- & \frac{1}{\sqrt{2}}(\omega_\mu - \rho_\mu^0) & K_\mu^{*0} \\ K_\mu^{*-} & \bar{K}_\mu^{*0} & \phi_\mu \end{pmatrix}, \quad (11)$$

respectively. In a similar manner, we can write the pseudoscalar nonet ( $\Pi$ ) and pseudovector nonet ( $A_\mu$ ). The total effective Lagrangian density in the chiral  $SU(3)$  quark mean field model is written as

$$\mathcal{L}_{\text{eff}} = \mathcal{L}_{q0} + \mathcal{L}_{qm} + \mathcal{L}_{\Sigma\Sigma} + \mathcal{L}_{VV} + \mathcal{L}_{\chi SB} + \mathcal{L}_{\Delta m} + \mathcal{L}_c, \quad (12)$$

where  $\mathcal{L}_{q0} = \bar{q}i\gamma^\mu\partial_\mu q$  represents the kinetic term of the Lagrangian density, and  $\mathcal{L}_{qm}$  is the chiral  $SU(3)$ -invariant quark-meson interaction term and is written as

$$\begin{aligned} \mathcal{L}_{qm} &= g_s (\bar{\Psi}_L M \Psi_R + \bar{\Psi}_R M^\dagger \Psi_L) \\ &\quad - g_v (\bar{\Psi}_L \gamma^\mu l_\mu \Psi_L + \bar{\Psi}_R \gamma^\mu r_\mu \Psi_R) \\ &= \frac{g_s}{\sqrt{2}} \bar{\Psi} \left( \sum_{a=0}^8 s_a \lambda_a + i\gamma^5 \sum_{a=0}^8 p_a \lambda_a \right) \Psi \\ &\quad - \frac{g_v}{2\sqrt{2}} \bar{\Psi} \left( \gamma^\mu \sum_{a=0}^8 v_\mu^a \lambda_a - \gamma^\mu \gamma^5 \sum_{a=0}^8 a_\mu^a \lambda_a \right) \Psi, \end{aligned} \quad (13)$$

where  $\Psi = \begin{pmatrix} u \\ d \\ s \end{pmatrix}$ . The chiral-invariant scalar and vector meson self interaction terms  $\mathcal{L}_{\Sigma\Sigma}$  and  $\mathcal{L}_{VV}$ , within the mean field approximation [52], are written as

$$\begin{aligned} \mathcal{L}_{\Sigma\Sigma} &= -\frac{1}{2} k_0 \chi^2 (\sigma^2 + \zeta^2) + k_1 (\sigma^2 + \zeta^2)^2 + k_2 \left( \frac{\sigma^4}{2} + \zeta^4 \right) \\ &\quad + k_3 \chi \sigma^2 \zeta - k_4 \chi^4 - \frac{1}{4} \chi^4 \ln \frac{\chi^4}{\chi_0^4} + \frac{\xi}{3} \chi^4 \ln \frac{\sigma^2 \zeta}{\sigma_0^2 \zeta_0}, \end{aligned} \quad (14)$$

and

$$\mathcal{L}_{VV} = \frac{1}{2} \frac{\chi^2}{\chi_0^2} (m_\omega^2 \omega^2) + g_4 \omega^4, \quad (15)$$

respectively. The constants  $k_0, k_1, k_2, k_3$  and  $k_4$  in Eq. (14) are determined using the  $\pi$  meson mass ( $m_\pi$ ), K meson mass ( $m_K$ ) and the average mass of  $\eta$  and  $\eta'$  mesons [41]. The other parameters, i.e.,  $\xi$ , the vacuum value of the dilaton field,  $\chi_0$ , and, the coupling constant  $g_4$ , are chosen so as to fit the effective nucleon mass reasonably. Further, the value of the parameter  $\xi$  originating from the logarithmic term used in scalar meson self interaction Lagrangian density can be obtained using the QCD  $\beta$ -function at one loop level, for three colors and three flavors [43]. The Lagrangian density  $\mathcal{L}_{\chi SB}$  in Eq. (12) is introduced to incorporate non-vanishing pseudoscalar meson masses and it satisfies the partially conserved axial-vector current relations for  $\pi$  and K mesons [41, 52, 53]. We have

$$\mathcal{L}_{\chi SB} = \frac{\chi^2}{\chi_0^2} \left[ m_\pi^2 F_\pi \sigma + \left( \sqrt{2} m_K^2 F_K - \frac{m_\pi^2}{\sqrt{2}} F_\pi \right) \zeta \right], \quad (16)$$

where  $F_\pi$  and  $F_K$  are pion and kaon decay constants, respectively. The masses of u, d and s quarks are generated by the vacuum expectation values of  $\sigma$  and  $\zeta$  meson scalar fields. In order to find the constituent strange quark mass correctly, an additional mass term which would explicitly break the chiral symmetry is written in Eq. (12). This term can be expressed as

$$\mathcal{L}_{\Delta m} = -m_1 \bar{\Psi} S_1 \Psi, \quad (17)$$

where  $m_1$  is the additional mass term. The strange quark matrix operator  $S_1$  is defined as  $S_1 = \frac{1}{3}(I - \lambda_8 \sqrt{3}) = \text{diag}(0, 0, 1)$ . Thus, the relations for vacuum masses of quarks are

$$m_u = m_d = -g_\sigma^a \sigma_0 = -\frac{g_s}{\sqrt{2}} \sigma_0, \quad \text{and} \quad m_s = -g_\zeta^s \zeta_0 + m_1. \quad (18)$$

The values of the coupling constant  $g_s$  and additional mass term  $m_1$  in Eq. (18) can be calculated by taking  $m_u = m_d = 313$  MeV and  $m_s = 490$  MeV as the vacuum masses of quarks. The interaction between the quarks and vector mesons leads to [52]

$$\begin{aligned} \frac{g_s}{\sqrt{2}} &= g_\sigma^u = g_\sigma^d = \frac{1}{\sqrt{2}} g_\zeta^s, \\ g_\sigma^s &= g_\zeta^u = g_\zeta^d = 0, \\ g_\omega^u &= g_\omega^d = g_\omega^a, \\ g_\omega^s &= 0. \end{aligned} \quad (19)$$

Quarks are confined in baryons by a confining scalar-vector potential, given by [52]

$$\chi_c(r) = \frac{1}{4} k_c r^2 (1 + \gamma^0). \quad (20)$$

The coupling constant  $k_c$  is taken to be 100 MeV.fm<sup>-2</sup>. The corresponding Lagrangian density is written as

$$\mathcal{L}_c = -\bar{\Psi} \chi_c \Psi. \quad (21)$$

In order to investigate the properties of nuclear matter at finite temperature and density, we will use the mean field approximation [52]. The Dirac equation under the influence of a meson mean field, for the quark field  $\Psi_{qj}$  is given by

$$\left[ -i \vec{\alpha} \cdot \vec{\nabla} + \chi_c(r) + \beta m_q^* \right] \Psi_{qj} = e_q^* \Psi_{qj}, \quad (22)$$

where the subscripts  $q$  and  $j$  denote the quark  $q$  ( $q = u, d, s$ ) in a baryon of type  $j$  ( $j = N, \Lambda, \Sigma, \Xi$ ) and  $\vec{\alpha}$ ,  $\beta$  are the usual Dirac matrices. The effective quark mass  $m_q^*$  is defined as

$$m_q^* = -g_\sigma^q \sigma - g_\zeta^q \zeta + m_{q0}, \quad (23)$$

where  $m_{q0} = m_1$  is zero for non-strange  $u$  and  $d$  quarks, whereas for the strange  $s$  quark  $m_{q0} = m_1 = 29$  MeV. The effective energy of a particular quark under the influence of a meson field is given as  $e_q^* = e_q - g_\omega^i \omega - g_\phi^i \phi$  [41, 52]. For the confining potential defined by Eq. (20), the analytical expression for the effective energy of quark  $e_q^*$  will be

$$e_q^* = m_q^* + \frac{3\sqrt{k_c}}{\sqrt{2(e_q^* + m_q^*)}}. \quad (24)$$

The effective mass of baryons can be calculated from the effective quark masses  $m_q^*$ , using the relation

$$M_j^* = \sqrt{E_j^{*2} - \langle p_{j\text{cm}}^* \rangle}, \quad (25)$$

where the effective energy of the  $j^{\text{th}}$  baryon in the nuclear medium is given as

$$E_j^* = \sum_q n_{qj} e_q^* + E_{j\text{spin}}. \quad (26)$$

Further,  $E_{j\text{spin}}$  is the correction to baryon energy due to the spin-spin interaction of constituent quarks and takes the values

$$\begin{aligned} E_{N\text{spin}} &= -477 \text{ MeV}, \quad E_{\Lambda\text{spin}} = -756.9 \text{ MeV}, \\ E_{\Sigma\text{spin}} &= -531 \text{ MeV}, \quad E_{\Xi\text{spin}} = -705 \text{ MeV}. \end{aligned}$$

These values are determined to fit the respective vacuum values of baryon masses. In Eq. (25),  $\langle p_{j\text{cm}}^* \rangle$  is the spurious center of mass motion [66, 68]. To study the equations of motion for mesons at finite temperature and density, we consider the thermopotential as

$$\begin{aligned} \Omega &= - \sum_{B=N, \Lambda, \Sigma, \Xi} \frac{g_j k_B T}{(2\pi)^3} \\ &\int_0^\infty d^3 k \left\{ \ln(1 + e^{-[E^*(k) - \nu_B]/k_B T}) \right. \\ &\left. + \ln(1 + e^{-[E^*(k) + \nu_B]/k_B T}) \right\} - \mathcal{L}_M, \end{aligned} \quad (27)$$

where

$$\mathcal{L}_M = \mathcal{L}_{\Sigma\Sigma} + \mathcal{L}_{VV} + \mathcal{L}_{\chi SB}, \quad (28)$$

and  $g_j$  is the degeneracy of the  $j^{\text{th}}$  baryon ( $g_{N, \Xi} = 2$ ,  $g_\Lambda = 1$ ,  $g_\Sigma = 3$ ) and  $E^*(k) = \sqrt{M_j^{*2} + k^2}$ . We can relate the quantity  $\nu_B$  to the chemical potential  $\mu_B$  as [41, 52, 53]

$$\nu_B = \mu_B - g_j^i \omega. \quad (29)$$

The equations of motion for scalar fields  $\sigma$ ,  $\zeta$ , the dilaton field,  $\chi$ , and the vector field  $\omega$  are calculated from the thermodynamical potential and are expressed respectively as

$$\begin{aligned} k_0 \chi^2 \sigma - 4k_1 (\sigma^2 + \zeta^2) \sigma - 2k_2 \sigma^3 - 2k_3 \chi \sigma \zeta - \frac{2\xi}{3\sigma} \chi^4 \\ + \frac{\chi^2}{\chi_0^2} m_\pi^2 F_\pi - \left( \frac{\chi}{\chi_0} \right)^2 m_\omega \omega^2 \frac{\partial m_\omega}{\partial \sigma} + \frac{\partial M_N^*}{\partial \sigma} \langle \bar{\psi}_N \psi_N \rangle = 0, \end{aligned} \quad (30)$$

$$\begin{aligned} k_0 \chi^2 \zeta - 4k_1 (\sigma^2 + \zeta^2) \zeta - 4k_2 \zeta^3 - k_3 \chi \sigma^2 - \frac{\xi}{3\zeta} \chi^4 \\ + \frac{\chi^2}{\chi_0^2} \left( \sqrt{2} m_K^2 F_K - \frac{1}{\sqrt{2}} m_\pi^2 F_\pi \right) = 0, \end{aligned} \quad (31)$$

$$\begin{aligned} k_0 \chi^2 (\sigma^2 + \zeta^2) - k_3 \chi \sigma^2 \zeta + \left( 4k_4 + 1 - 4 \ln \frac{\chi^4}{\chi_0^4} + \frac{4\xi}{3} \ln \frac{\sigma^2 \zeta}{\sigma_0^2 \zeta_0} \right) \chi^3 \\ + \frac{2\chi}{\chi_0^2} \left[ m_\pi^2 F_\pi \sigma + \left( \sqrt{2} m_K^2 F_K - \frac{1}{\sqrt{2}} m_\pi^2 F_\pi \right) \zeta \right] - \frac{\chi}{\chi_0^2} m_\omega^2 \omega^2 = 0, \end{aligned} \quad (32)$$

and

$$\frac{\chi^2}{\chi_0^2}(m_\omega^2\omega^2)+4g_4\omega^3=g_\omega^N\langle\psi_N^\dagger\psi_N\rangle. \quad (33)$$

In Eq. (30),  $\langle\bar{\psi}_N\psi_N\rangle$  is the scalar density of nucleons and is given by

$$\langle\bar{\psi}_N\psi_N\rangle=\frac{g_N}{2\pi^2}\int_0^\infty dk\frac{k^2M_j^*}{\sqrt{M_j^{*2}+k^2}}[n_n(k)+\bar{n}_n(k)+n_p(k)+\bar{n}_p(k)]. \quad (34)$$

The number density of nucleons in Eq. (33) is given as

$$\langle\psi_N^\dagger\psi_N\rangle=\frac{g_N}{2\pi^2}\int_0^\infty dk k^2[n_n(k)+\bar{n}_n(k)+n_p(k)+\bar{n}_p(k)], \quad (35)$$

where  $n_n(k)$  and  $n_p(k)$  are the neutron and proton distributions, and  $\bar{n}_n(k)$  and  $\bar{n}_p(k)$  are the anti-neutron and anti-proton distributions, respectively and are defined as

$$n_\tau(k)=\{\exp[(E^*(k)-\nu_B)/k_B T]+1\}^{-1}, \quad (36)$$

$$\bar{n}_\tau(k)=\{\exp[(E^*(k)+\nu_B)/k_B T]+1\}^{-1}, \quad (\tau=n,p). \quad (37)$$

The vacuum expectation values of the meson fields  $\sigma_0$  and  $\zeta_0$  are constrained because of spontaneous breaking of chiral symmetry and are represented in terms of pion and kaon leptonic decay constants as

$$\sigma_0=-F_\pi, \quad \zeta_0=\frac{1}{\sqrt{2}}(F_\pi-2F_K). \quad (38)$$

For  $F_\pi=92.8$  MeV and  $F_K=115$  MeV, the vacuum values of the  $\sigma$  and  $\zeta$  fields are  $\sigma_0=-92.8$  MeV and  $\zeta_0=-96.5$  MeV respectively.

## 2.2 Magnetic Moment of Baryons

So far we have used the chiral  $SU(3)$  quark mean field model using effective Lagrangian density for the various interactions for calculating the effective mass of

$$q=\begin{pmatrix} u \\ d \\ s \end{pmatrix}, \quad \Phi=\begin{pmatrix} \frac{\pi^0}{\sqrt{2}}+\varpi\frac{\eta}{\sqrt{6}}+\tau\frac{\eta'}{\sqrt{3}} & \pi^+ \\ \pi^- & \varepsilon K^+ \\ \varepsilon K^- & -\frac{\pi^0}{\sqrt{2}}+\varpi\frac{\eta}{\sqrt{6}}+\tau\frac{\eta'}{\sqrt{3}} \\ & \varepsilon\bar{K}^0 & -\varpi\frac{2\eta}{\sqrt{6}}+\tau\frac{\eta'}{\sqrt{3}} \end{pmatrix}.$$

In the above,  $\varepsilon$ ,  $\varpi$  are symmetry breaking parameters. Further, the parameter  $\tau=g_1/g_8$ , where  $g_1$  and  $g_8$  are the coupling constants for the singlet and octet GBs, respectively. However, in accordance with New Muon Collaboration [82] calculations we have used the value of  $\tau$  obtained according to the relation

$$\tau=-0.7-\frac{\varpi}{2} \quad (44)$$

$SU(3)$  symmetry breaking is introduced by considering  $m_s>m_{u,d}$ , as well as by considering the masses of GBs to be nondegenerate ( $m_{K,\eta}>m_\pi$ ) [35, 47, 55, 56]. The

constituent quarks. In order to calculate the explicit contributions of the valence and sea quark effects to the magnetic moment of baryons, we follow the idea of the chiral quark model initiated by Weinberg [50] and developed by Manohar and Georgi [51]. The model incorporates the ideas of confinement and chiral symmetry breaking. The massless quarks acquire mass through spontaneous breaking of chiral symmetry. The basic process in this approach is the emission of a GB, which further splits into a  $q\bar{q}$  pair, e.g.,

$$q_\pm\rightarrow\text{GB}^0+q'_\mp\rightarrow(q\bar{q}')+q'_\mp, \quad (39)$$

where  $q\bar{q}'+q'$  constitute the ‘sea quarks’ [35, 47, 55, 56]. Within the QCD confinement scale and chiral symmetry breaking, the constituent quarks, octet of GBs and the weakly interacting gluons are the appropriate degrees of freedom [58]. The effective Lagrangian in this region is given as

$$\mathcal{L}_{\text{interaction}}=\bar{\psi}(i\not{D}+V)\psi+i g_A\bar{\psi}A\gamma^5\psi+\dots, \quad (40)$$

where  $g_A$  is the axial vector coupling constant. In the low energy limit gluonic degrees can be neglected. Hence, the above effective interaction Lagrangian with GBs and quarks in leading order is written as

$$\mathcal{L}_{\text{interaction}}=-\frac{g_A}{f_\pi}\bar{\psi}\partial_\mu\Phi\gamma^\mu\gamma^5\psi. \quad (41)$$

Using Dirac’s equation ( $i\gamma^\mu\partial_\mu-m_q$ ) $q=0$ , the effective Lagrangian describing the interaction between quarks and a nonet of GBs consisting of an octet and a singlet, and suppressing all the space-time structure to the lowest order, can be expressed as

$$\mathcal{L}=g_s\bar{q}\Phi q, \quad (42)$$

with

$$\Phi=\begin{pmatrix} \pi^+ & \varepsilon K^+ \\ -\frac{\pi^0}{\sqrt{2}}+\varpi\frac{\eta}{\sqrt{6}}+\tau\frac{\eta'}{\sqrt{3}} & \varepsilon K^0 \\ \varepsilon\bar{K}^0 & -\varpi\frac{2\eta}{\sqrt{6}}+\tau\frac{\eta'}{\sqrt{3}} \end{pmatrix}. \quad (43)$$

Octet baryon wave functions include singlet and triplet states and the gluon exchange forces generates the mixing between them. Following the Cheng and Li mechanism [14], the magnetic moment of baryons, including the contributions from valence quarks, sea quarks and the orbital angular momentum of sea quarks, can be written as

$$\mu(B)_{\text{total}}=\mu(B)_{\text{val}}+\mu(B)_{\text{sea}}+\mu(B)_{\text{orbital}}, \quad (45)$$

where  $\mu(B)_{\text{val}}$  and  $\mu(B)_{\text{sea}}$  represent the contributions from valence and sea quarks, respectively. The valence and sea contributions in terms of quark spin polariza-

tions can be written as

$$\mu(B)_{\text{val}} = \sum_{q=u,d,s} \Delta q_{\text{val}} \mu_q \quad \text{and} \quad \mu(B)_{\text{sea}} = \sum_{q=u,d,s} \Delta q_{\text{sea}} \mu_q, \quad (46)$$

where  $\Delta q_{\text{val}}$  and  $\Delta q_{\text{sea}}$  are the spin polarizations due to valence and sea quarks, respectively. Quark spin polarization is defined as

$$\Delta q = q^+ - q^- + q^{\bar{+}} - q^{\bar{-}}, \quad (47)$$

where  $q^+(q^{\bar{+}})$  and  $q^-(q^{\bar{-}})$  is number of quarks (anti-quarks) with spin up and down, respectively. The sum of  $\Delta q$ 's gives the total spin carried by the quarks. The spin structure of the baryon is given as

$$\widehat{B} = \langle B | N | B \rangle,$$

where  $N$  is the number operator corresponding to different quark flavors with spins up and down and is expressed as

$$N = n_{u^+} u^+ + n_{u^-} u^- + n_{d^+} d^+ + n_{d^-} d^- + n_{s^+} s^+ + n_{s^-} s^-,$$

with the coefficient of  $q^\pm$  giving the number of  $q^\pm$  quarks. The calculation of the number of up and down quarks in a specific baryon has been explicitly done in Ref. [54]. The sea quark polarization  $\Delta q_{\text{sea}}$  can be expressed in terms of symmetry breaking parameters  $\varepsilon$  and  $\varpi$ . For example, in the case of the proton,  $\Delta u_{\text{sea}}$ ,  $\Delta d_{\text{sea}}$  and  $\Delta s_{\text{sea}}$  are defined as

$$\begin{aligned} \Delta u_{\text{sea}} &= -\frac{a}{3} \left[ 7 + 4\varepsilon^2 + \frac{4}{3}\varpi^2 + \frac{8}{3}\tau^2 \right], \\ \Delta d_{\text{sea}} &= -\frac{a}{3} \left[ 2 - \varepsilon^2 - \frac{1}{3}\varpi^2 - \frac{2}{3}\tau^2 \right], \\ \Delta s_{\text{sea}} &= -a\varepsilon^2, \end{aligned} \quad (48)$$

respectively. The pion fluctuation parameter  $a$  is taken to be 0.1 in the symmetric limit [67]. Similarly,  $\Delta q_{\text{sea}}$  is defined for other baryons in Refs. [14, 54].

The values of effective magnetic moments of constituent quarks ( $\mu_q$ ) can be calculated following the naive quark model formula given as  $\mu_q = \frac{e_q}{2m_q}$ , where  $m_q$  and  $e_q$  are the mass and electric charge of the quark, respectively. This formula lacks consistency for calculation of magnetic moments of relativistically confined quarks [59]. Further, the non-relativistic quark momenta are required to be very small ( $p_q^2 \ll (350 \text{ MeV})^2$ ) for quark masses in the range of 313 MeV and higher. Hence, in order to include the quark confinement effect on magnetic moment [59, 71] along with the relativistic correction to quark magnetic moments (introduced in quarks by using the medium-modified quark masses obtained in the chiral  $SU(3)$  quark mean field model, which considers quarks as Dirac particles), the mass term in the formula for quark magnetic moment is replaced by the expectation value of effective quark mass  $m_q^{\text{B}}$ , which can be further expressed

in terms of effective baryon mass following the formula

$$2m_q^{\text{B}} = M_B^* + m_q + \Delta M,$$

where  $M_B^*$  is the effective mass of the baryon,  $m_q (\approx 0)$  is the current quark mass and  $\Delta M$  is the confinement correction term [59].

Following the above formalism, the equations to calculate effective magnetic moments  $\mu_q$  of constituent quarks are now given as

$$\mu_d = -\left(1 - \frac{\Delta M}{M_B^*}\right), \quad \mu_s = -\frac{m_u^*}{m_s^*} \left(1 - \frac{\Delta M}{M_B^*}\right), \quad \mu_u = -2\mu_d. \quad (49)$$

Eq. (49) gives the known mass-adjusted magnetic moments of constituent quarks [58].  $M_B^*$  is obtained in Eq. (25). To include the quark confinement effect it is replaced by  $M_B^* + \Delta M$ ,  $\Delta M$  being the difference between the experimental vacuum mass of the baryon ( $M_{\text{vac}}$ ) and the effective mass of the baryon  $M_B^*$ , i. e.,  $\Delta M = M_{\text{vac}} - M_B^*$ .

The contribution from orbital angular momentum of sea quarks to an octet baryon of type B(xxy) is given as

$$\mu(B(xxy))_{\text{orbit}} = \Delta x [\mu(x^+ \rightarrow)] + \Delta y [\mu(y^+ \rightarrow)], \quad (50)$$

and for a baryon of type B(xyz) it is

$$\begin{aligned} \mu(B(xyz))_{\text{orbit}} &= \Delta x [\mu(x^+ \rightarrow)] + \Delta y [\mu(y^+ \rightarrow)] \\ &\quad + \Delta z [\mu(z^+ \rightarrow)]. \end{aligned} \quad (51)$$

In Eqs. (50) and (51), the symbols  $x$ ,  $y$  and  $z$  correspond to any of the constituent quarks of the baryon, i.e., u, d or s, and  $\Delta x$ ,  $\Delta y$  and  $\Delta z$  represent the quark spin polarizations due to valence quarks. The expressions for orbital moments of u, d and s, i.e.,  $\mu(u^+ \rightarrow)$ ,  $\mu(d^+ \rightarrow)$  and  $\mu(s^+ \rightarrow)$  in terms of effective masses of quarks (in units of nuclear magneton  $\mu_N$ ) are given as

$$\begin{aligned} \mu(u^+ \rightarrow) &= a \left[ \frac{-m_\pi^2 + 3m_u^{*2}}{2m_\pi(m_u^* + m_\pi)} - \frac{\varepsilon^2(m_K^2 - 3m_u^{*2})}{2m_K(m_u^* + m_K)} \right] \\ &\quad + a \left[ \frac{(3 + \varpi^2 + 2\tau^2)m_{\eta'}^2}{6m_{\eta'}(m_u^* + m_{\eta'})} \right], \end{aligned} \quad (52)$$

$$\begin{aligned} \mu(d^+ \rightarrow) &= a \frac{m_u^*}{m_d^*} \left[ \frac{2m_\pi^2 - 3m_d^{*2}}{2m_\pi(m_d^* + m_\pi)} - \frac{\varepsilon^2 m_K^2}{2m_K(m_d^* + m_K)} \right] \\ &\quad - a \frac{m_u^*}{m_d^*} \left[ \frac{(3 + \varpi^2 + 2\tau^2)m_{\eta'}^2}{12m_{\eta'}(m_u^* + m_{\eta'})} \right], \end{aligned} \quad (53)$$

$$\mu(s^+ \rightarrow) = a \frac{m_u^*}{m_s^*} \left[ \frac{\varepsilon^2(m_K^2 - 3m_s^{*2})}{2m_K(m_s^* + m_K)} - \frac{(2\varpi^2 + \tau^2)m_{\eta'}^2}{6m_{\eta'}(m_u^* + m_{\eta'})} \right]. \quad (54)$$

These contributions can be calculated as done in Ref. [54]. However, they are worth noting in order to consider the medium modification of sea quark spin polarization  $\Delta q_{\text{sea}}$  and orbital angular momentum contributions  $\mu(u^+ \rightarrow)$ ,  $\mu(d^+ \rightarrow)$  and  $\mu(s^+ \rightarrow)$ . The parameters  $\varepsilon$  and  $\varpi$  appear in the linear representation of octet scalar

density [84]. The linear combination of these parameters gives the familiar ‘F’ and ‘D’ coefficients. These parameters can be expressed in terms of medium modified quark and baryon masses as

$$\varepsilon = \frac{M_{\Sigma}^* - M_{\Xi}^*}{\left(\frac{m_u^* + m_d^* - 2m_s^*}{2}\right)}, \quad (55)$$

and

$$\varpi = \frac{M_{\Sigma}^* - M_N^*}{\left(\frac{m_u^* + m_d^* - 2m_s^*}{2}\right)}. \quad (56)$$

These two parameters along with  $\tau$ , given by Eq. (44), lead to medium modification of sea quark polarizations

and orbital moments. Physically  $\varepsilon^2 a$ ,  $\varpi^2 a$  and  $\tau^2 a$  respectively denote the probabilities of transitions  $u(d) \rightarrow s+K^-$ ,  $u(d,s) \rightarrow u(d,s)+\eta$  and  $u(d,s) \rightarrow u(d,s)+\eta'$ . Note that orbital angular momentum contribution is calculated using the parameters  $\varepsilon, \varpi$  and  $\tau$  along with the masses of GBs. The GB contributions are dominated by the pion contribution as compared to contributions from other GBs.

### 3 Numerical results

In this section we present the results of our investigation on magnetic moment of baryons at finite density and temperature of medium. The various parameters used in the present work are tabulated in Table 1.

Table 1. Values of various parameters used in this work [41].

$m_u/\text{MeV}$	$m_d/\text{MeV}$	$m_s/\text{MeV}$	$m_\pi/\text{MeV}$	$m_K/\text{MeV}$	$k_0$	$k_1$	$k_2$	$k_3$	$k_4$
313	313	490	139	494	4.94	2.12	-10.16	-5.38	-0.06
$\sigma_0/\text{MeV}$	$\zeta_0/\text{MeV}$	$\chi_0/\text{MeV}$	$\xi$	$\rho_0/\text{fm}^{-3}$	$g_\sigma^u = g_\sigma^d$	$g_\sigma^s$	$g_\zeta^u = g_\zeta^d$	$g_\zeta^s$	$g_4$
-92.8	-96.5	254.6	6/33	0.16	3.37	0	0	4.77	37.4

From Eq. (49) it is clear that the value of magnetic moment of constituent quarks depends on the effective masses of the quarks and baryons, which in turn depend on the scalar fields  $\sigma$  and  $\zeta$  through Eqs. (23), (24), (25) and (26). In order to study the effect of density on the scalar fields  $\sigma$  and  $\zeta$ , in the left-hand panel of Fig. (1) we plot the scalar field  $\sigma$  against nuclear matter density  $\rho_B$  (in units of nuclear saturation density), at different temperatures of the medium  $T = 0, 50, 100$  and  $150$  MeV. We observe that the magnitude of the  $\sigma$  field decreases sharply with the rise of nuclear matter density below  $\rho_B = 2\rho_0$ . For densities more than  $2\rho_0$ , the decrease in magnitude of the  $\sigma$  field as a function of  $\rho_B$  is slow. For example, at  $T = 0$  MeV, the  $\sigma$  field changes by 73% as  $\rho_B$  is changed from zero to  $2\rho_0$ . However, as the baryonic density increases from  $2\rho_0$  to  $4\rho_0$ , the magnitude of the scalar field  $\sigma$  changes by 50%. The amount of this decrease in the value of  $\sigma$  field is even less at higher densities. Considering the effect of temperature, we observe that the magnitude of the  $\sigma$  field decreases less rapidly as a function of density at higher temperatures of medium than at lower temperatures. However, at  $\rho_B = 0$ , with the rise of temperature the magnitudes of scalar fields decrease. At a given finite density of the medium, the magnitude of the  $\sigma$  field increases with increasing temperature. For example, at nuclear saturation density ( $\rho_B = \rho_0$ ), the magnitudes of the  $\sigma$  fields are 45.71, 49.3 and 52.96 MeV at  $T = 0, 50$  and  $100$  MeV, respectively. This is explained as follows. At  $\rho_B = 0$ , the thermal distribution functions alone effect the variation of fields. However, with the rise of density, another contribution

starts coming from higher momentum states, which provides an opposite effect to the variation of scalar fields [70]. Thus, due to these two contributions, i.e., thermal distribution function and higher momentum states, the behavior of the scalar fields is reversed with the rise of temperature at finite value of density of medium, as compared to its behavior at zero baryonic density.

In the right-hand panel of Fig. 1, we have plotted the variation of the  $\zeta$  field with nuclear matter density at temperatures  $T = 0, 50, 100$  and  $150$  MeV. One can clearly see that the magnitude of the  $\zeta$  field decreases very slowly as a function of density as compared to scalar field  $\sigma$ , indicating that there is strong correlation between the nucleons and the  $\sigma$  field. However, the  $\zeta$  field changes very slowly because it does not depend on the non-strange quark content of the medium. For example, at  $T = 0$  MeV, there is a decrease of only 20% in magnitude of the  $\zeta$  field as  $\rho_B$  increases from 0 to  $2\rho_0$ . Further, on calculating the variation in the magnitude of  $\zeta$  field at different temperatures, the decrease in magnitude as a function of density is less for higher temperatures than for  $T = 0$  MeV. This difference increases for higher values of nuclear matter density. For example, at  $\rho_B = \rho_0$ , there is a difference of 2.25 MeV in the magnitudes of  $\zeta$  field at  $T = 0$  MeV and  $T = 100$  MeV. However, at  $\rho_B = 5\rho_0$ , this difference in the values of  $\zeta$  field changes to 5.6 MeV. At nuclear saturation density, the magnitude of the  $\zeta$  field decreases by only 2% with the rise of temperature from  $T = 0$  MeV to  $T = 100$  MeV. However, at  $\rho_B = 5\rho_0$  the above value of percentage change shifts to 6%.

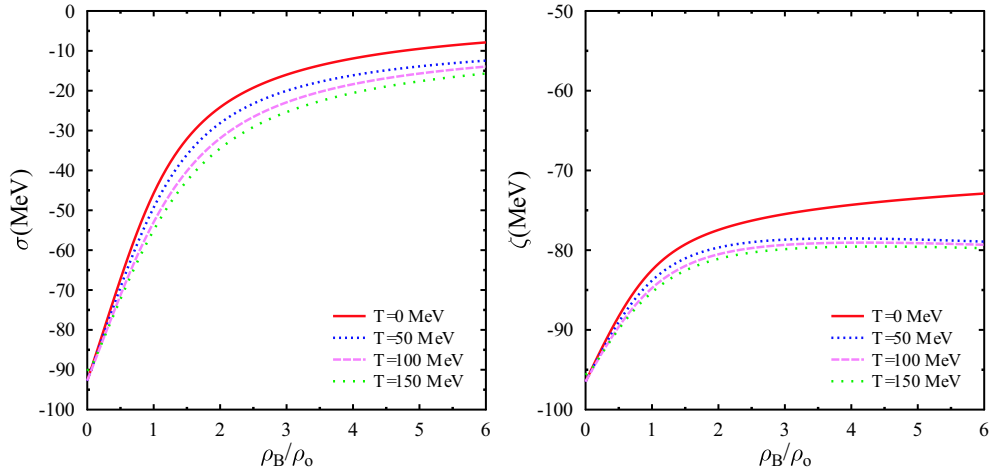


Fig. 1. (color online)  $\sigma$  and  $\zeta$  fields (at  $T = 0, 50, 100$  and  $150$  MeV) versus baryonic density (in units of nuclear saturation density  $\rho_0$ ).

Using the above calculated values of the  $\sigma$  and  $\zeta$  fields, the in-medium quark masses,  $m_q^*$ , can be evaluated using Eq. (23). Note that in this work, the non-strange quark masses ( $m_u^*$  and  $m_d^*$ ) depend on the scalar meson field  $\sigma$  only. Because the coupling constant  $g_\zeta^u = g_\zeta^d = 0$ , in Eq. (23)  $\zeta$  is eliminated for  $m_u^*$  and  $m_d^*$ . As the magnitude of the  $\sigma$  field decreases sharply with increasing density, especially at densities up to  $2\rho_0$ , there is a steep decrease in the effective mass of non-strange quarks at a lower value of density medium for a fixed temperature. At higher nuclear matter density, however, the decrease in effective quark mass is much less. For example, at temperature  $T = 0$  MeV, the effective mass of a u (or d) quark at  $\rho_B = 3\rho_0, 4\rho_0$  and  $5\rho_0$  decreases to 53.92, 40.19 and 32.01 MeV, respectively, from its vacuum value of 313 MeV.

For a given finite value of baryonic density, the effective mass of non-strange quarks increases with the increase in the temperature of the nuclear medium. For example, at  $\rho_B = \rho_0$ , the values of  $m_u^*$  are observed to be 154.2, 165.9, 178.2 and 185 MeV at  $T = 0, 50, 100$  and 150 MeV, respectively. However, at zero density, the effective masses of non-strange quarks decrease with increasing temperature. The reason for this behavior is the dynamical generation of quark masses by coupling with the scalar fields  $\sigma$  and  $\zeta$ .

Further, the magnitudes of scalar fields decrease with increasing density, at  $T = 0$  MeV. Therefore, the value of  $m_u^*$  (and  $m_d^*$ ) also decreases with increasing baryonic density, at  $T = 0$  MeV. The probable cause for this behavior of effective quark masses is chiral symmetry restoration at higher densities, which has been reported in the literature, by using the chiral hadronic model, in the quark degrees of freedom [39].

It has been seen that  $m_s^*$  decreases less rapidly than  $m_u^*$  and  $m_d^*$ , when plotted as a function of baryonic den-

sity, at given values of temperature. At temperature  $T = 0$  MeV, as the density of the medium increases from 0 to  $\rho_0$ ,  $m_s^*$  decreases by about 14%. Further, at higher values of density but the same temperature ( $T = 0$  MeV),  $m_s^*$  decreases very slowly. The reason for this behavior of  $m_s^*$  at finite baryonic density is its dependence on the scalar  $\zeta$  field, and the absence of coupling between the s-quark and  $\sigma$  field as  $g_\sigma^s = 0$ .

One also finds that the effective mass of the s quark increases with increasing temperature, at a given finite value of density. For example, at  $\rho_B = \rho_0$ , the effective mass of the s quark is 422.5, 427.5 and 432.5 MeV at temperatures  $T = 0, 50$  and 100 MeV, respectively. Further, for higher values of density, the increase in effective mass of the s quark becomes slow with increasing temperature. For example, at  $\rho_B = 2\rho_0$ , for the rise of temperature from  $T = 0$  to  $T = 50$  MeV and from  $T = 50$  to  $T = 100$  MeV, the effective mass of the s quark increases by 9.7 MeV and 4 MeV, respectively.

Also, we observe that the effective mass of the s quark decreases with increasing density up to baryonic density  $\rho_B = 4\rho_0$ , at finite temperature. However, on further increase of density above  $4\rho_0$ , at the same value of finite temperature, the effective mass of the s quark starts increasing. The increase in constituent quark masses with increase in density of the medium above  $4\rho_0$ , at given finite temperature, could be due to deconfinement phase transition at higher density [61].

Now we discuss the medium modification of octet baryon masses calculated using Eq. (25), through the medium-modified masses of quarks in Eq. (23). In Fig. 2, we plot the medium-modified octet baryon masses ( $M_i^*$ ,  $i = N, \Sigma, \Xi, \Lambda$ ) as a function of density at temperatures  $T = 0, 50, 100$  and 150 MeV. We see that the variation of effective masses of constituent quarks greatly affects the medium modification of baryon masses. For ex-



ample, in the case of nucleons with non-strange quark content only, there is a steep decrease in the effective baryonic masses. Our calculations show that at  $T = 0$  MeV, as the density increases from  $\rho_B = 0$  to  $\rho_0$ , the effective mass of nucleons decreases by 41% from its vacuum value. Similar behavior has been reported in the literature [62], where the effective field calculations show a decrease of 30% in effective nucleon masses for a rise of density from  $\rho_B = 0$  to  $\rho_0$  at  $T = 0$  MeV. This difference is due to the model dependence of quark and baryon masses. Further, at  $T = 0$  MeV, the effective nucleon mass decreases to 41%, 36%, 33% and 31% of its vacuum value at  $\rho_B = 2\rho_0, 3\rho_0, 4\rho_0$  and  $5\rho_0$ , respectively.

As compared to nucleons, the in-medium masses of strange baryons decrease less rapidly as a function of density of the medium, at a given temperature. For example, at  $T = 0$  MeV, for a rise of density from  $\rho_B = 0$  to  $\rho_0$ , there is a decrease of 25%, 28% and 16% in the effective masses of the  $\Sigma$ ,  $\Lambda$  and  $\Xi$  baryons, respectively.

One can also observe that, with the rise of temperature, at a given value of density of the medium, the effective masses of baryons increase. For example, at  $\rho_B = \rho_0$ , the effective mass of nucleons increases by 10% as the temperature rises from  $T = 0$  to  $T = 100$  MeV. Further, at  $\rho_B = \rho_0$ , the effective masses of  $\Sigma$ ,  $\Lambda$  and  $\Xi$

baryons increase by 5%, 5.5% and 3%, respectively, with the rise of temperature from  $T = 0$  MeV to  $T = 100$  MeV. One can see that the increase of effective masses of strange baryon masses with the rise of temperature, at given finite value of density of the medium, is slow compared to the increase in effective masses of the nucleons. The reason for this behavior of effective masses of octet baryons is their dependence on the constituent quark masses. The effective masses of the u and d quarks increase significantly, whereas the effective mass of the s quark increases slowly with the rise of temperature, at finite value of density. This is why the increase in effective masses of strange baryons slows with increase in strangeness content of the baryon.

Now we will discuss the medium modification of baryon magnetic moments of octet baryons. In Fig. 3, we plot the magnetic moment of octet baryons with density at temperatures  $T = 0, 50, 100$  and  $150$  MeV. In Tables 2 and 3, we have given the observed values of medium-modified magnetic moments of octet baryons, at temperatures  $T = 0$  MeV and  $100$  MeV, respectively. The values are calculated for densities  $\rho_B = 0, \rho_0$  and  $4\rho_0$ . Note that in Table (2) we have also given the experimentally observed vacuum values of magnetic moment of octet baryons.

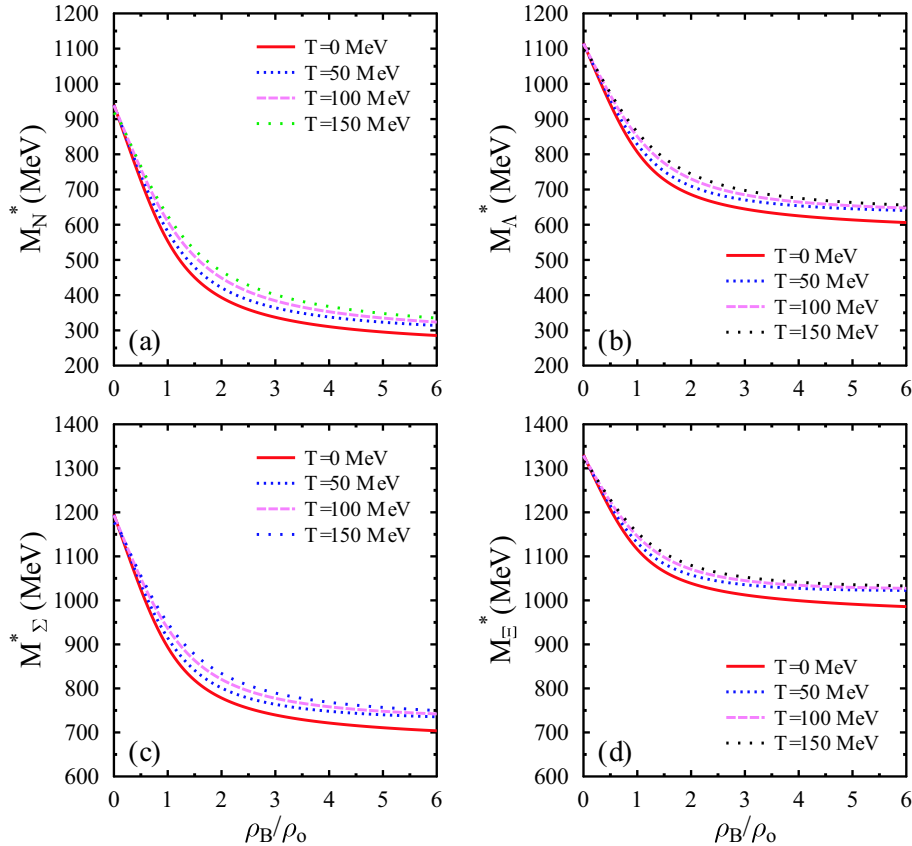


Fig. 2. (color online) Effective masses of octet baryons (at  $T = 0, 50, 100$  and  $150$  MeV) versus baryonic density (in units of nuclear saturation density  $\rho_0$ ).

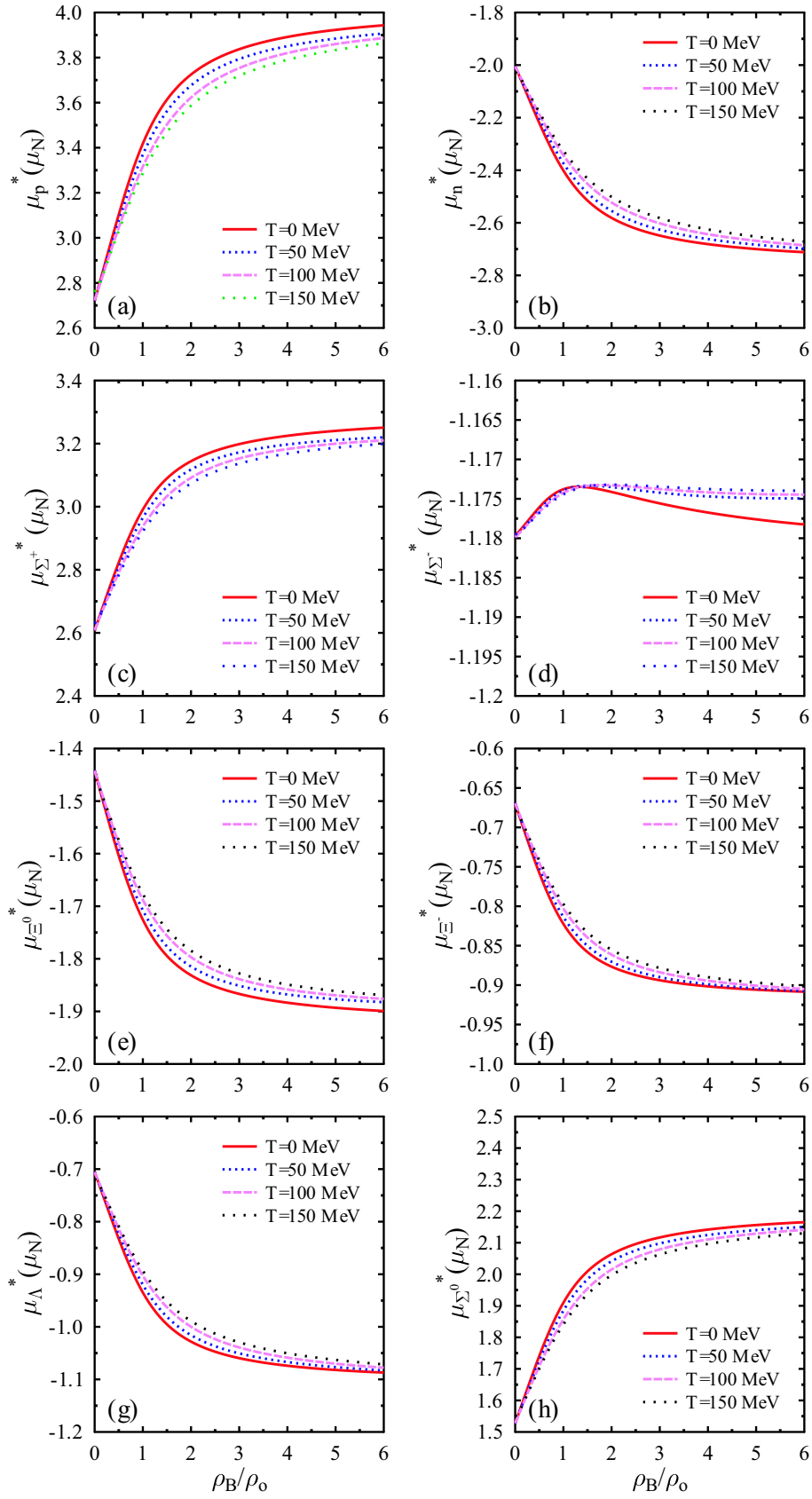


Fig. 3. (color online) Magnetic moment of octet baryons (at  $T = 0, 50, 100$  and  $150$  MeV) versus baryonic density (in units of nuclear saturation density  $\rho_0$ ).

Table 2. Effective magnetic moments of octet baryons at  $T = 0$  MeV and  $\rho_B=0, \rho_0$  and  $4\rho_0$ .

	data [85]		$\rho_B=0$			$\rho_B=\rho_0$				$\rho_B=4\rho_0$			
	$\mu_{total}$	$\mu_{val}$	$\mu_{sea}$	$\mu_{orbital}$	$\mu_{total}$	$\mu_{val}$	$\mu_{sea}$	$\mu_{orbital}$	$\mu_{total}$	$\mu_{val}$	$\mu_{sea}$	$\mu_{orbital}$	$\mu_{total}$
$\mu_p^*(\mu_N)$	2.792	2.994	-0.724	0.450	2.72	4.232	-0.985	0.172	3.418	5.008	-1.129	0.013	3.892
$\mu_n^*(\mu_N)$	-1.913	-1.996	0.414	-0.422	-2.004	-2.821	0.583	-0.166	-2.401	-3.338	0.656	0.001	-2.681
$\mu_{\Sigma^+}^*(\mu_N)$	2.458	3.002	-0.776	0.381	2.607	3.758	-0.914	0.146	2.991	4.190	-0.980	0.015	3.225
$\mu_{\Sigma^-}^*(\mu_N)$	-1.160	-1.001	0.137	-0.316	-1.18	-1.253	0.201	-0.122	-1.174	-1.397	0.215	0.005	-1.177
$\mu_{\Sigma^0}^*(\mu_N)$	-1.610	-1.386	-0.078	-0.256	-1.721	-1.909	-0.029	-0.096	-2.035	-2.312	-0.016	-0.003	-2.331
$\mu_{\Xi^0}^*(\mu_N)$	-1.250	-2.000	0.614	-0.055	-1.441	-2.323	0.623	-0.025	-1.726	-2.498	0.621	-0.006	-1.883
$\mu_{\Xi^-}^*(\mu_N)$	-0.650	-1.000	0.386	-0.055	-0.669	-1.162	0.365	-0.025	-0.822	-1.249	0.354	-0.006	-0.902
$\mu_{\Lambda}^*(\mu_N)$	-0.613	-0.664	0.336	-0.042	-0.705	-0.952	0.362	-0.019	-0.935	-1.070	0.370	-0.004	-1.074

Table 3. Effective magnetic moments of octet baryons at  $T = 100$  MeV and  $\rho_B=0, \rho_0$  and  $4\rho_0$ .

	$\rho_B=0$				$\rho_B=\rho_0$				$\rho_B=4\rho_0$			
	$\mu_{val}$	$\mu_{sea}$	$\mu_{orbital}$	$\mu_{total}$	$\mu_{val}$	$\mu_{sea}$	$\mu_{orbital}$	$\mu_{total}$	$\mu_{val}$	$\mu_{sea}$	$\mu_{orbital}$	$\mu_{total}$
$\mu_p^*(\mu_N)$	3.001	-0.727	0.449	2.723	4.053	-0.948	0.212	3.316	4.873	-1.090	0.037	3.820
$\mu_n^*(\mu_N)$	-2.001	0.416	-0.421	-2.005	-2.702	0.560	-0.201	-2.343	-3.248	0.631	-0.026	-2.643
$\mu_{\Sigma^+}^*(\mu_N)$	3.007	-0.778	0.380	2.609	3.651	-0.894	0.180	2.937	4.098	-0.950	0.035	3.183
$\mu_{\Sigma^-}^*(\mu_N)$	-1.002	0.138	-0.316	-1.18	-1.217	0.193	-0.150	-1.174	-1.366	0.207	-0.015	-1.174
$\mu_{\Sigma^0}^*(\mu_N)$	-1.389	-0.080	-0.255	-1.724	-1.826	-0.033	-0.119	-1.979	-2.228	0.001	-0.018	-2.244
$\mu_{\Xi^0}^*(\mu_N)$	-2.004	0.625	-0.055	-1.442	-2.278	0.620	-0.029	-1.688	-2.446	0.596	-0.009	-1.858
$\mu_{\Xi^-}^*(\mu_N)$	-1.002	0.388	-0.055	-1.228	-1.139	0.366	-0.029	-1.546	-1.223	0.337	-0.009	-1.771
$\mu_{\Lambda}^*(\mu_N)$	-1.002	0.338	-0.042	-0.706	-1.238	0.357	-0.022	-0.903	-1.405	0.352	-0.007	-1.059

If we consider the effect of valence quarks only, the vacuum value of magnetic moment of baryons as calculated in our model comes out to be larger than the experimental values. For example, at  $\rho_B=0$  and  $T = 0$  MeV, considering the valence quark effect only, the magnetic moment of proton comes out to be  $2.994\mu_N$ , which is more than the experimental value of the magnetic moment of the proton in vacuum, i.e.,  $2.79\mu_N$  [54]. In order to get more realistic values of magnetic moments, we have included the contribution from the ‘Goldstone Boson Exchange’ effect, also known as the sea quark effect, whose contribution to the magnetic moment of baryons is opposite to that of the valence quark contribution. Following the Cheng and Li mechanism [14], we have also considered the effect of the contribution of the orbital angular momentum of sea quarks [54]. It is important to note that the sea quark effect gives an opposite contribution to total magnetic moment of baryons as compared to the valence quark effect, whereas the contribution from orbital angular momentum of sea quarks is of the same sign as that from the valence quark effect.

The observed behavior of magnetic moment of baryons may be directly related to the spin decomposition of nucleons and other baryons, which is one of the key problems in nucleon structure physics [72–74]. The spin sum rule to calculate proton spin  $J$  can be expressed as

$$J = \frac{1}{2}\Sigma + L_q + \Delta g + L_g,$$

where  $\Sigma$  is the quark spin,  $L_q$  is quark angular momen-

tum,  $\Delta g$  is the contribution from gluon spin and  $L_g$  is the orbital angular momentum of the gluon. Experimental observations by the European Muon Collaboration in deep inelastic scattering experiments have shown that the valence quarks in the proton carry only about 30% of the total spin of the proton [75]. The remaining spin may come from the angular momentum part of quark spin, the gluon spin part, and the orbital angular momentum of gluons in the total spin of proton. The quark spin ( $\Sigma$ ) may further split into the contribution from valence and sea quarks as  $\Sigma = \Sigma_V + \Sigma_S$ . Gluon spin and orbital angular momentum of gluon parts are very small as indicated by different experimental studies [76, 77], and can be neglected at present. In the present model, the splitting of a quark into quark and GB leads to a flip of quark spin, which means that the quarks produced through this process which constitute the ‘quark sea’ are eventually polarized in the opposite direction to that of the valence quarks. The contribution from the orbital angular momentum part is, however, of the same sign as that of the valence quarks. Further, in the case of the proton, due to flavor asymmetry, the effect of polarization of two u quarks is more than the effect of polarization of one d quark. This leads to the fact that in the case of the proton, the total contribution from sea quark polarization is more than the opposite contribution from the orbital angular momentum part. This behavior for the spin sum rule has been reported in the literature [78–81], and the magnetic moments calculated in the present work also follow the same behavior.

On comparing the values in Tables 2 and 3, we find that at  $\rho_B = 0$ , the magnetic moments of the baryons are almost the same at  $T = 0$  MeV and  $T = 100$  MeV. This means that at zero baryonic density there is negligible effect of increasing temperature on effective magnetic moments of baryons. However, at finite densities, there is a noticeable change in the values of magnetic moments of baryons, especially in case of nucleons.

We find that with the rise of density of the medium at  $T = 0$  MeV as well as 100 MeV, the magnitude of sea quark polarizations decrease. For example, at  $T = 0$  MeV, the magnitude of  $\Delta u_{\text{sea}}$  in the case of the proton, as given in Eq. (48), is found to be 0.165, 0.134 and 0.129 at  $\rho_B = 0, \rho_0$  and  $4\rho_0$ , respectively. This is due to medium modification of the symmetry breaking parameters  $\varepsilon$  and  $\varpi$  along with parameter  $\tau$ . However, if we do not consider medium modification of these parameters, the value of  $\Delta u_{\text{sea}}$  remains equal to its vacuum value at all the densities. However, with the rise of density of the medium at the same temperature, the total effective magnetic moments vary significantly because of medium modification of sea quark polarization. For example, at  $T = 0$  MeV and  $\rho_B = \rho_0$ ,  $\mu_p = 3.418\mu_N$  and  $\mu_{\Xi^0} = -1.726\mu_N$  with medium modified sea quark polarization, whereas, with constant value (vacuum value) of sea quark polarization at all densities, these values comes out to be 3.450 and  $-1.902\mu_N$ , respectively. If we consider the effect of increasing temperature on  $\Delta u_{\text{sea}}$ , we find that for a given finite value of density of the medium,  $\Delta u_{\text{sea}}$  is negligibly affected by the rise of temperature. For example, at  $T = 100$  MeV, the magnitude of  $\Delta u_{\text{sea}}$  is 0.165, 0.137 and 0.128 at  $\rho_B = 0, \rho_0$  and  $4\rho_0$ , respectively. Further, one can see that both at  $T = 0$  MeV and 100 MeV, the contribution of orbital angular momentum of sea quarks decreases with increasing density.

We also see that with the increase of strangeness content the increase in magnitude of effective magnetic moment of baryon is less. This is because  $m_s^*$  varies very slowly with density at a given temperature. Further, at given finite temperature, the effective magnetic moments are not very sensitive to quark mass variation for higher densities. Our calculations show that at temperature  $T = 0$  MeV, for the rise of density of nuclear medium from  $\rho_B = 0$  to  $\rho_0$ , the effective magnetic moment of the proton increases by 26%. However, for further increase in the density of the medium, at the same temperature, the rise of magnetic moment of the proton becomes slow. For example, at  $T = 0$  MeV, for a rise of density from  $2\rho_0$  to  $6\rho_0$ , the effective magnetic moment rises by 20%. A cloudy bag model prediction shows enhancement of magnetic moment with the rise of nuclear matter density from  $\rho_B = 0$  to  $\rho_0$  in the range of 2%–20% [48]. Further, models like the constituent quark model, QMC model pion cloud, Skyrme model, chiral quark soliton model

and NJL model predict enhancement up to 10%. In our calculations this enhancement is 26%, which is quite large compared to these previous predictions. This is due to the model dependence of effective baryon masses and hence magnetic moments.

Further, in Table 2, we see that at  $T = 0$  MeV, for rise of density from  $\rho_B = 0$  to nuclear saturation density, the magnitude of effective magnetic moment increases by 15%, 0.5% and 25% in case of the  $\Sigma^+$ ,  $\Sigma^-$  and  $\Sigma^0$  baryons respectively. The very small change in effective magnetic moment of  $\Sigma^-$  is due to comparable contributions from the sea quark effect and orbital angular momentum of sea quarks, whereas for the other baryons these contributions do not completely cancel each other out. In the case of the  $\Xi^0$ ,  $\Xi^-$  baryons, this increase in magnitude of magnetic moments is 20% and 23%, respectively. In particular, for the  $\Lambda$  baryon, the magnitude of effective magnetic moment increases by 32%. This behavior is completely different from that in the case of the QMC calculations, where the magnitude of  $\mu_\Lambda^*$  decreases by 0.7%. However, in the case of the modified QMC calculations, the magnitude increases by 10% [48]. A possible reason for this is model dependence of effective quark masses. In the present work, the modification of magnetic moments of baryons depends on medium modification of constituent quark masses, whereas in Ref. [48], the modification of magnetic moments was derived from modification of the bag radius.

To understand more explicitly the effect of temperature of the medium on magnetic moments of octet baryons, in Fig. 4 we plot the effective magnetic moments of baryons as a function of temperature, at  $\rho_B = 0$ ,  $\rho_0$  and  $4\rho_0$ .

We note that at a given density of medium, with increasing temperature, the magnetic moments of baryons increase slightly. For example, at  $\rho_B = 0$ , the effective values of magnetic moment of the proton are observed to be  $2.720\mu_N$ ,  $2.722\mu_N$ ,  $2.723\mu_N$ ,  $2.760\mu_N$  at temperatures,  $T = 0, 50, 100$  and  $150$  MeV, respectively. Hence, the variation in effective magnetic moment of baryons as a function of temperature is negligible at zero density up to critical temperature. These results are in good agreement with those obtained in Ref. [60, 61], where magnetic moments of nucleons were calculated using the quark sigma model. However, as the temperature reaches its critical value there is a steep increase in the magnitude of effective magnetic moments. This can be attributed to a second order phase transition above critical temperature.

At finite density, the change in effective value of magnetic moment of baryons is almost negligible as a function of temperature compared to that at zero density. These results can be explained as follows. From Eqs. (46) and (49), we find that the effective magnetic

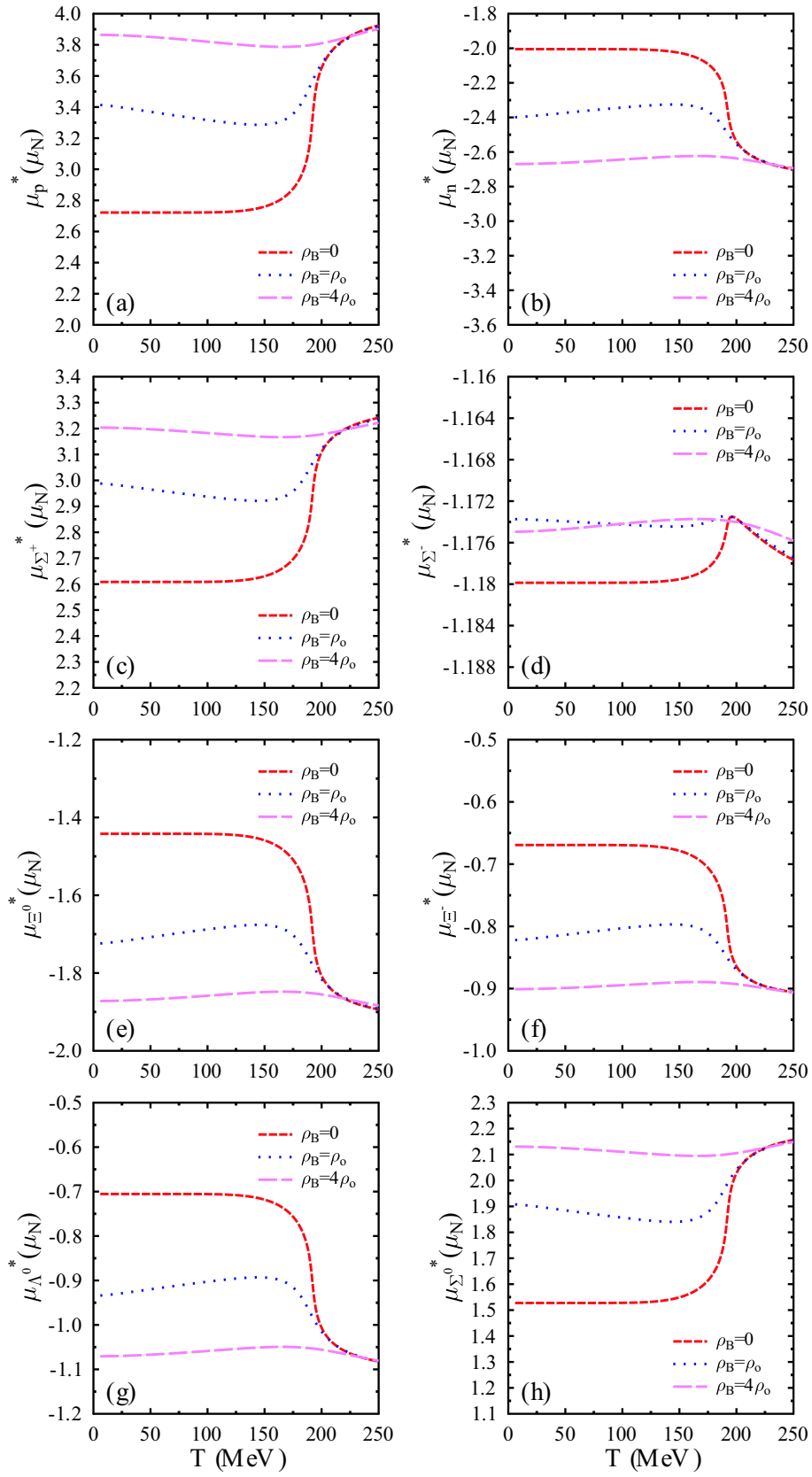


Fig. 4. (color online) Magnetic moments of baryons as a function of temperature at  $\rho_B=0, \rho_0$  and  $4\rho_0$ .

moments of baryons are inversely proportional to the medium-modified values of constituent quark masses. At  $\rho_B=0$ , the effective quark mass remains almost the same with increasing temperature up to a certain value of temperature, because the thermal distribution functions alone affect the self energies of constituent quarks and hence decrease the effective quark masses (increasing the effective magnetic moment of baryons). However, with increasing density, another contribution starts coming from higher momentum states, due to which the effective magnetic moments start decreasing (as the effective masses of quarks increase) [70]. Further, for still higher densities, i.e.,  $4\rho_0$  or more, the variation of effective magnetic moment of baryons become insensitive to the variation in effective mass of constituent quarks. This can be due to a second order phase transition at higher densities and temperatures. This observation is further justified by those expected in Ref. [65], where medium-modified baryonic magnetic moments using a modified quark meson coupling model were calculated.

## 4 Summary

We have studied the magnetic moment of baryons at finite density and temperature of symmetric nuclear matter by using the chiral  $SU(3)$  quark mean field approach. The explicit contributions from valence quarks, sea quarks and orbital angular momentum of sea quarks have also been considered to give a better insight into medium modification of magnetic moments. Considering only the valence quark effect gives magnetic moments more than the experimental data for vacuum values. The sea quark effect gives the opposite contribution to the total effective magnetic moments, as compared to the valence quarks. However, considering the sea quark effect

alone decreases the vacuum values to lower than those in experimental data [54]. Hence, in order to get more realistic vacuum values we have considered the contribution from orbital angular momentum of the sea quarks, which gives a considerable opposite contribution to the magnetic moments compared to that from the sea quarks, especially at lower densities, and a small contribution at higher densities.

The magnetic moments of nucleons are found to vary greatly as a function of density at low temperatures. At higher temperatures, however, this variation of magnetic moment becomes slow. The magnetic moments of strange baryons are found to vary slowly with density as well as temperature as compared to those of non-strange baryons. This is because of the dependence of magnetic moments on medium-modified values of the strange quark mass, which vary very slowly because of small coupling with the scalar meson field. Further, the variation of effective magnetic moments of baryons as a function of temperature is negligible for nuclear matter density higher than  $4\rho_0$ . This indicates a second order phase transition at higher densities [69].

It was found in Ref. [83] that the pion loop correction shows only a minute contribution to anomalous magnetic moments of baryons. However, we have derived the medium modification of sea quark polarization through medium modification of symmetry breaking parameters  $\varepsilon$  and  $\varpi$ . The results can be further improved by including contributions from effects from relativistic and exchange currents [57], pion cloud contributions [63] and the effects of confinement [59] etc., which can contribute effectively in obtaining the correct vacuum values of magnetic moments of octet baryons, and for further analysis of magnetic moments in the presence of a medium.

## References

- 1 J. Beringer et al, Phys. Rev. D, **86**: 010001 (2012)
- 2 J. Ashman et al (EMC Collaboration), Phys. Lett. B, **206**: 364 (1988); J. Ashman et al (EMC Collaboration), Nucl. Phys. B, **328**: 1 (1989)
- 3 V. Friese, Nucl. Phys. A, **774**: 377 (2005)
- 4 Johann M. Heuser, Nucl. Phys. A, **830**: 563 (2009)
- 5 G. Aad et al, Phys. Rev. D, **89**: 092009 (2014)
- 6 P. Senges, Acta Physica Polonica B, **37**: 1 (2006)
- 7 S. Sahu, Revista Mexicana De Fisica, **48**: 48 (2002)
- 8 F. Schlumpf, Phys. Rev. D, **48**: 4478 (1993),
- 9 W. R. B. de Araujo et al, Brazilian Journal of Physics, **34**: 871 (2004)
- 10 E. J. Hackett-Jones, D. B. Leinweber, and A. W. Thomas, Phys. Lett. B, **489**: 143 (2000)
- 11 J. G. Contreras, R. Huerta, Revista Mexicana De Fisica, **50**: 490 (2004)
- 12 H. E. Jun, Dong Yu-Bing, Commun. Theor. Phys., **43**: 139 (2005)
- 13 Lalit K. Sharma, C. Mai, J. Sci., **34**: 13 (2007)
- 14 T. P. Cheng and Ling Fong Li, Phys. Rev. Lett., **74**: 2872 (1995)
- 15 J. Linde, T. Ohlsson, and H. Snellman, Phys. Rev. D, **57**: 092009 (1998)
- 16 T. Draper, Keh-Fei Liu, Nucl. Phys. A, **527**: 531 (1991)
- 17 D. B. Leinweber, R. M. Woloshyn, Nucl. Phys. B, Proc. Suppl., **20**: 463 (1991)
- 18 M. Z. Navgran, Maryam, Int. Sci. index, **59**: 1174 (2011)
- 19 C. Y. Ryu, M. K. Cheoun, and C. H. Hyun, Journal of Korean Physical Society, **54**: 1448 (2009)
- 20 B. O. Kerbikov, Yu. A. Simonov, Phys. Rev. D, **62**: 093016 (2000).
- 21 L. S. Geng, J. M. Camalich, L. A. Ruso, and M. J. Vicente Vacas, Phys. Rev. Lett., **101**: 222002 (2008)
- 22 L. S. Geng, J. M. Camalich, and M. J. Vicente Vacas, Phys. Rev. D, **80**: 034027 (2009)
- 23 J. Gasser, H. Leutwyler, Nucl. Phys. B, **250**: 465 (1985)
- 24 J. Gasser, M. E. Sainio and A. Svarc, Nucl. Phys. B, **307**: 779 (1988)
- 25 S. Scherer, Adv. Nucl. Phys., **27**: 277 (2003)
- 26 E. E. Jenkins et al, Phys. Lett. B, **302**: 482 (1993)
- 27 L. Durand, P. Ha, Phys. Rev. D, **58**: 013010 (1998)

- 28 S. J. Puglia, M. J. Ramsey-Musolf, Phys. Rev. D, **62**: 034010 (2000)
- 29 U. G. Meissner, S. Steininger, Nucl. Phys. B, **499**: 349 (1997)
- 30 J. J. Aubert et al, Phys. Lett. B, **123**: 275 (1983)
- 31 P. J. Mulders, Phys. Reports, **185**: 83 (1990)
- 32 J. D. Walecka, Ann. Phys. (N. Y.), **83**: 491 (1974)
- 33 N. Petropoulos, arxiv:hep-ph/0402136
- 34 P. Wang et al, Phys. Rev. C, **70**: 015202 (2004)
- 35 H. Q. Song, R. K. Su, Phys. Lett. B, **358**: 179 (1995)
- 36 G. A. Miller, Phys. Rev. C, **66**: 032201 (2002)
- 37 M. Buballa, Phys. Rept., **407**: 205 (2005)
- 38 Gustavo A. Contera, Phys. Lett. B, **661**: 113 (2008)
- 39 P. Rau et al, J. Phys. G: Nucl. Part. Phys., **40**: 085001 (2013)
- 40 T. Hatsuda, T. Kunihiro, Phys. Rept., **247**: 221 (1994)
- 41 P. Wang, Z. Zong-Ye and Y. You-Wen, Commun. Theor. Phys., **36**: 71 (2001)
- 42 H. Shen and H. Toki, Phys. Rev. C, **61**: 045205 (2000)
- 43 P. Papazoglou, D. Zschesche, S. Schramm, J. Schaffner-Bielich, H. Stöcker, and W. Greiner, Phys. Rev. C, **59**: 411 (1999)
- 44 M. A. Thaler, R. A. Schneides, W. Weise, Phys. Rev. C, **69**: 035210 (2003)
- 45 R. F. Wagenbrunn et al, Phys. Rev. B, **33**: 511 (2001)
- 46 S. Capstick, B. D. Keister, arXiv:nucl-th/9611055
- 47 J. Linde, T. Ohlsson, and Hakan Snellman, Phys. Rev. D, **57**: 452 (1998)
- 48 C. Y. Ryu, C. H. Hyun, T. S. Park, and S. W. Hong, Phys. Lett. B, **674**: 122 (2009)
- 49 H. J. Lipkin, arxiv:hep-ph/9911261
- 50 S. Weinberg, Physica A, **96**: 327 (1979)
- 51 A. Manohar, H. Georgi, Nucl. Phys. B, **234**: 189 (1984)
- 52 P. Wang, Z. Y. Song et al, Nucl. Phys. A, **688**: 791 (2001)
- 53 P. Wang et al, Nucl. Phys. A, **744**: 273 (2004)
- 54 H. Dahiya, M. Gupta, Phys. Rev. D, **64**: 014013 (2001)
- 55 T. P. Cheng, L. F. Li, Phys. Rev. Lett., **80**: 2789 (1998)
- 56 T. P. Cheng, Ling Fong Li, Phys. Rev. D, **57**: 344 (1998)
- 57 M. Gupta, N. Kaur, Phys. Rev. D, **28**: 534 (1983)
- 58 A. Gridhar, H. Dahiya, M. Randhawa, Phys. Rev. D, **92**(3): 033012 (2015)
- 59 Ikuro S. Sogami, N. Oh'yamaguchi, Phys. Rev. Lett., **54**: 2295 (1985); Kuang-Ta Chao, Phys. Rev. D, **41**: 920 (1990)
- 60 C. V. Christov, E. R. Arriola, and K. Goeke, Nucl. Phys. A, **556**: 641 (1993); M. Arneodo et al, Phys. Rev. D, **50**: R1 (1994)
- 61 M. Abu-Shady, A. K. Abu-Nab, American Journal of Physics and App., **46**: 1 (2014)
- 62 J. W. Holt, M. Rho, and W. Weise, arxiv:1411.6681v2 [nucl-th]
- 63 S. Theberge and A. W. Thomas, Phys. Rev. D, **25**: 284 (1982); J. Cohen and H.J. Weber, Phys. Lett. B, **165**: 229 (1985)
- 64 L. Durand and P. Ha, Phys. Rev. D, **58**: 013010 (1998)
- 65 C. Y. Ryu and K. S. Kim, Phys. Rev. C, **82**: 025804 (2010)
- 66 N. Barik, B. K. Dash, Phys. Rev. D, **31**: 7 (1985)
- 67 T. P. Cheng and L. F. Li, Phys. Rev. Lett., **74**: 2872 (1995); T. P. Cheng and L. F. Li, Phys. Rev. D, **59**: 097503 (1999); X. Song and V. Gupta, Phys. Rev. D, **49**: 2211 (1994)
- 68 N. Barik et al, Phys. Rev. C, **88**: 015206 (2013)
- 69 P. Wang et al, Phys. Rev. C, **72**: 045801 (2005)
- 70 A. Mishra et al, Eur. Phys. J. A, **41**: 205 (2009); **98**: 631 (1997)
- 71 M. Gupta, J. Phys. G, **16**: L213 (1990)
- 72 A. J. Buchmann, E. M. Henley, Phys. Rev. D, **83**: 096011 (2010)
- 73 L. M. Sehgal, Phys. Rev. D, **10**: 1663 (1974)
- 74 X. Ji, Phys. Rev. Lett., **78**: 610 (1997).
- 75 J. M. S. Rana, H. Dahiya, M. Gupta, AIP Conference Proceedings, **63**: 1056 (2008)
- 76 A. W. Thomas, Int. J. Mod. Phys. E, **18**: 1116 (2009)
- 77 S. J. Brodsky, S. Gardner, Phys. Lett. B, **643**: 22 (2006)
- 78 H. Dahiya, M. Randhawa, Phys. Rev. D, **93**: 114030 (2016)
- 79 X. Song, arxiv:hep-ph/0012295v3
- 80 L. F. Li and T. P. Cheng, Chinese Journal of Physics, **35**: 6 (1997)
- 81 L. F. Li and T. P. Cheng, Phys. Rev. Lett., **74**: 15 (1995)
- 82 New Muon Collaboration, P. Amaudruz et al: Phys. Rev. Lett., **66**: 2712 (1991)
- 83 L. Ya. Glozman, D. O. Riska, Phys. Lett. B, **459**: 49 (1999)
- 84 L. F. Li and T. P. Cheng, arxiv:hep-ph/9709293
- 85 W-M Yao, C. Amsler, D. Asner et al, Particle Data Group. J. Phys. G, **33**: 1 (2006)